

Force-induced Unbinding Dynamics in a Multidimensional Free Energy Landscape[†]Changbong Hyeon^a

Department of Chemistry, Chung-Ang University, Seoul 156-756, Korea. E-mail: hyeoncb@kias.re.kr

Received November 30, 2011, Accepted January 5, 2012

We examined theory for force-induced unbinding on a two-dimensional free energy surface where the internal dynamics of biomolecules is coupled with the rupture process under constant tension f . We show that only if the transition state ensemble is narrow and activation barrier is high, the f -dependent rupture rate in the 2D potential surface can faithfully be described using an effective 1D energy profile.

Key Words : Force dynamics, Kramers equation, Multidimensional surface, Hydrodynamic coupling

Introduction

Since the birth of chemical dynamics,^{1,2} broad classes of simple reactions have been described using a physically suitable one dimensional reaction coordinate.³⁻⁵ It is, however, well appreciated that such a description often fails to capture the dynamics of complex systems such as the folding of proteins or RNA.^{6,7} Interestingly, the response of biological molecules to mechanical force (f) is often described using a one dimensional (1D) free energy profile ($F(R)$) with, R , the molecular extension that is conjugate to f being the natural reaction coordinate.⁸ Use of R as the reaction coordinate is appropriate if the relaxation dynamics associated with all other degrees of freedom are much faster than the dynamics associated with R . The celebrated phenomenological Bell model⁹ and related microscopic models,¹⁰⁻¹³ which assume that bond rupture dynamics or forced unfolding of proteins and RNA can be described using $F(R)$, have apparently been adequate in interpreting a number of single molecule experiments. When subject to a tension the transverse fluctuations of the molecule are suppressed, which makes it plausible that the dynamics (forced-unfolding or bond rupture) occurs along an effective 1D free energy profile. A broader validity of the adequacy of $F(R)$ was established in the context of a RNA hairpin dynamics subject to f .¹⁴ By using the calculated free energy profile at $f=f_m$, the force at which the probabilities of being in the folded and unfolded states are equal, it was shown that a Bell-type model can be used to quantitatively predict the dynamics at other f values.¹⁴ It is important to decipher whether energy landscape description based on R alone suffices to describe the force dynamics of biomolecules that, in principle, takes place in a multidimensional surface.

Here, we studied the f -dependent unbinding rates, $k_{2D}(f)$, over a barrier on a two dimensional free energy surface $F(x, y)$ in which the reaction coordinate x (describing unfolding or bond rupture) is coupled to an auxiliary

variable y . The following free energy surface (Fig. 1) is considered:

$$F(x, y) = -F^\ddagger \left[2 \left(\frac{x}{x^\ddagger} \right)^3 + 3 \left(\frac{x}{x^\ddagger} \right)^2 \right] - \kappa \left[\left(\frac{x}{x^\ddagger} \right) - b \right] y^2 - f x^\ddagger \left(\frac{x}{x^\ddagger} \right). \quad (1)$$

When $y=0$, $F(x, y)$ is reduced to the cubic potential that is popularly employed as a microscopic model potential by several group.¹⁰⁻¹² In $F(x, y)$, a harmonic potential is coupled in the orthogonal direction (y). Force along the x -direction, tilts the potential surface by $-f \cdot x$. In Eq. (1) the x -coordinate corresponds to the dynamics of R and the internal degrees of freedom is represented by motions along the y variable. (i) In the absence of tension ($f=0$), $F(x, y)$ has a local minimum at $x = -x^\ddagger$ and barrier top at $x=0$ along the $y=0$ axis. The height of potential barrier for the escape dynamics of a quasi-particle, which describes the rupture process, is F^\ddagger . The parameter b determines the 2D geometry of the transition barrier as well as of the local minimum at $(-x^\ddagger, 0)$. The transition barrier and local minimum become broad when b is small (see Fig. 1). However, the condition $b > 0$ should be retained for $F(x, y)$ to have a single saddle point. For $-1 < b \leq 0$, $E(x, y)$ forms two saddle points, and for $b \leq -1$ the local minimum at $x = -x^\ddagger$ is not stable. (ii) When $f \neq 0$, $F(x, 0)$ has

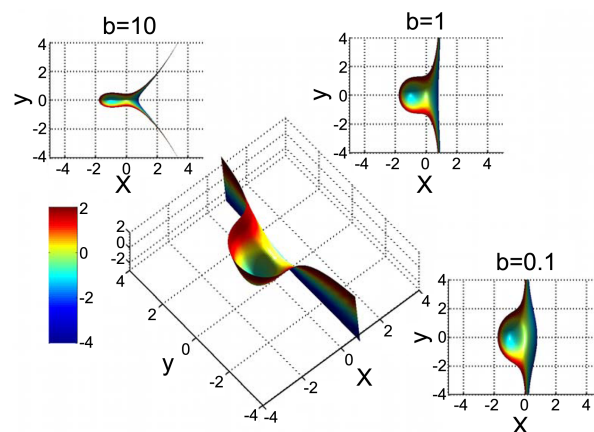


Figure 1. A two-dimensional energy surface using Eq. (1) with $f=0$, $\kappa=1$ and $\beta F^\ddagger=1$ and varying $b > 0$ values. x and y coordinates are scaled by x^\ddagger . The energy scale is color-coded in $k_B T$ unit.

[†]This paper is to commemorate Professor Kook Joe Shin's honourable retirement.

^aCurrent Address: School of Computational Sciences, Korea Institute for Advanced Study, Seoul 130-722, Korea

a tension-dependent local minimum at $x_0/x^\ddagger = (-1-\varepsilon_f)/2$ and a barrier at $x_b/x^\ddagger = (-1+\varepsilon_f)/2$ where $\varepsilon_f \equiv \sqrt{1-f/f_c}$ with $f_c = 3F^\ddagger/2x^\ddagger$. The barrier height at f is $F^\ddagger(f) = F(x_b, 0) - F(x_0, 0) = F^\ddagger \varepsilon_f^3$, which vanishes at $f = f_c$.

To calculate the f -dependent escape rate of the quasi-particle from the local minimum of $F(x, y)$ in the intermediate-to-high damping limit, we follow Langer's procedure,^{15,16} which extended the Kramers' theory to multidimension. The unfolding (or rupture) rate is

$$k = \frac{\lambda_+}{2\pi} \left[\frac{\det F^{(A)}}{|\det F^{(S)}|} \right]^{1/2} \exp(-\beta F^\ddagger(f)) \quad (2)$$

where total energy F is linearized at the saddle (S) and the potential minimum (A) using

$$F \approx F^{S,A} + \frac{1}{2} \sum_{i,j} \frac{\partial^2 F^{S,A}}{\partial \eta_i \partial \eta_j} (\eta_i - \eta_i^{S,A}) (\eta_j - \eta_j^{S,A}). \quad (3)$$

In the 2D problem associated with Eq. (1) the phase space points of the saddle and local minimum are $\{\eta^S\} = (x^S, y^S, p_x^S, p_y^S) = (x_b, 0, 0, 0)$ and $\{\eta^A\} = (x_0, 0, 0, 0)$, respectively. The rate constant k amounts to a flux-over-population expression from the steady state solution of a multidimensional Fokker-Planck equation. The λ_+ value corresponds to the deterministic growth rate at the saddle point from which the trajectory diverges exponentially along the reaction path. To calculate λ_+ , we use the Hamilton's equations of motion for each variable,

$$\dot{\eta}_i = - \sum_j M_{ij} \frac{\partial F}{\partial \eta_j} \quad (4)$$

and linearize the first derivative of E at S using,

$$\frac{\partial F}{\partial \eta_j} = \sum_k \left(\frac{\partial^2 F}{\partial \eta_j \partial \eta_k} \right)_S \delta \eta_k = \sum_k e_{jk} \delta \eta_k \quad (5)$$

where $\delta \eta_k^S \equiv \eta_k - \eta_k^S$ with $\eta_k = x, y, p_x, p_y$. Thus, $\{\eta\}$ satisfies the first order matrix equation

$$\dot{\eta}_i = - \sum_{j,k} M_{ij} e_{jk} \delta \eta_k \quad (6)$$

where

$$M = \begin{pmatrix} 0 & 0 & -1 & 0 \\ 0 & 0 & 0 & -1 \\ 1 & 0 & m\gamma_{xx} & 0 \\ 0 & 1 & 0 & m\gamma_{yy} \end{pmatrix} \quad (7)$$

and

$$e = \begin{pmatrix} -\frac{6F^\ddagger}{(x^\ddagger)^2} & 0 & 0 & 0 \\ 0 & \kappa(2b+1-\varepsilon_f) & 0 & 0 \\ 0 & 0 & 1/m & 0 \\ 0 & 0 & 0 & 1/m \end{pmatrix} \quad (8)$$

Among the four eigenvalues of Eq. (6), the expression for

the physically relevant one λ_+ is

$$\lambda_+(f) = -\frac{\gamma_{xx}}{2} + \sqrt{\left(\frac{\gamma_{xx}}{2}\right)^2 + \frac{6F^\ddagger}{m(x^\ddagger)^2} \varepsilon_f} \quad (9)$$

The determinants of the Hessian matrices at minimum (A ; +) and barrier top (S ; -) are calculated using

$$F^{(\pm)} = \begin{pmatrix} \pm \frac{6F^\ddagger}{(x^\ddagger)^2} \varepsilon_f & 0 & 0 & 0 \\ 0 & \kappa(2b+1 \pm \varepsilon_f) & 0 & 0 \\ 0 & 0 & 1/m & 0 \\ 0 & 0 & 0 & 1/m \end{pmatrix}, \quad (10)$$

where $F^{(+)} \equiv F^{(A)}$ and $F^{(-)} \equiv F^{(S)}$. Finally, the escape rate over the 2D model potential can be written as

$$k_{2D}(f) = \frac{\lambda_+}{2\pi} \sqrt{\frac{b+(1+\varepsilon_f)/2}{b+(1-\varepsilon_f)/2}} \exp(-\varepsilon_f^3 \beta F^\ddagger). \quad (11)$$

The stringent condition, $b > 0$, ensures that the potential has only a single saddle point. The parameter κ in Eq. (1), which defines the strength of the harmonic potential in y -direction, does not affect the barrier crossing kinetics in $k_{2D}(f)$ because of the symmetry of the cubic potential around the inflection point at $x = -x^\ddagger/2$. The rate at zero force ($k_0 \equiv k_{2D}(0)$) depends on b as

$$k_0(b) = \frac{\lambda_+(0)}{2\pi} \sqrt{\frac{b+1}{b}} \exp(-\beta F^\ddagger) \quad (12)$$

In the high damping limit ($\gamma_{xx} \gg 1$), the above expression is simplified to

$$\begin{aligned} k_{2D}(f) &= \frac{\varepsilon_f}{2\pi m \gamma_{xx}} \sqrt{\frac{b+(1+\varepsilon_f)/2}{b+(1-\varepsilon_f)/2}} \exp(-\varepsilon_f^3 \beta F^\ddagger) \\ &= D_{2D}(b, f) k_0(b) \varepsilon_f e^{(1-\varepsilon_f^3) \beta F^\ddagger} \\ &= D_{2D}(b, f) k_{1D}(f) \end{aligned} \quad (13)$$

where $k_0(b)$ is the rate at $f = 0$ and

$$D_{2D}(b, f) = \sqrt{\frac{b+(1+\varepsilon_f)/2}{b+(1-\varepsilon_f)/2}} \left(\frac{b}{b+1} \right)$$
 is the correction factor

for 2D reaction surface. $k_{1D}(f)$ is the rate expression for the 1D microscopic model ($\kappa = 0$ in Eq. (1)) with $\nu = 2/3$,^{10,11}

$$k_{1D}(f)/k_0(b) = \left(1 - \frac{\nu f x^\ddagger}{F^\ddagger} \right)^{1/\nu-1} \exp(\beta \Delta G^\ddagger \times [1 - (1 - \nu f x^\ddagger / F^\ddagger)^{1/\nu}]) \quad (14)$$

A few comments involving Eq. (13) are in place: (i) $D_{2D}(b, f) \approx 1$ is obtained either when $b \gg 1$ or when $\varepsilon_f \approx 1$. The deviation of $D_{2D}(b, f)$ from the unity becomes significant especially as b becomes smaller and f approaches the critical value ($f \rightarrow f_c$) so that the free energy barrier is about to vanish. (ii) The parameter b describes the geometry

around the saddle point and the local basin of attraction. When $b \gg 1$ the saddle point is sharply defined and transition state ensemble (TSE) is narrow. However, when $0 < b \ll 1$, both TSE and the local basin corresponding to the bound state are broad, leading to a large fluctuations orthogonal to the x -coordinate (Fig. 1). Description of force kinetics using $k_{1D}(f)$ fails when $0 < b \ll 1$ or the distinction between the transition state and the native basin (or bound state) is not transparent ($f/f_c \rightarrow 1$). In both scenarios the actual reaction paths deviate significantly from that determined along a predefined reaction coordinate. Under these conditions the one-dimensional reaction coordinate projected from multidimensional space cannot adequately describe the true dynamics even in the presence of f , which can usually moderate such fluctuations.

Instead of using the minimum path of the 2D surface as a 1D reaction coordinate, one can also consider the projection of 2D free energy surface by integrating the fluctuations in the y -coordinate, which allows us to define an effective 1D energy profile,

$$F^{\text{eff}}(x;b) = -\beta^{-1} \log \int_{-\delta}^{\delta} dy e^{-\beta F(x,y)} \\ \approx F(x,0) + \frac{1}{2} \beta^{-1} \log \left[\frac{\kappa \beta}{\pi} (b - x/x^\ddagger) \right]. \quad (15)$$

As shown in Figure 2, $F^{\text{eff}}(x;b)$ and $F(x;0)$ differs qualitatively when $b \rightarrow 0$ but only differs by a constant ($F^{\text{eff}}(x;b) - F(x;0) \approx 1/2 \beta^{-1} \log[\kappa \beta b / \pi]$) when $b > 1$. For $F^{\text{eff}}(x;b)$ with $b \rightarrow 0$ the effective transition barrier is smaller than in $F(x,0)$ (Fig. 2), which suggests that in the broad TSE the free energy barrier is lowered when the higher-dimensional free energy surface is projected onto one dimension. As a result the rate would increase provided that the prefactor for 1D-Kramers equation is nearly independent of b . In performing the integration to obtain the result in Eq. (15) we set $\delta = \infty$. This approximation is only valid for harmonic potential with a large κ or large b that results in rapid relaxation. For small κ or small b , motions along y -axis are slow and hence the δ

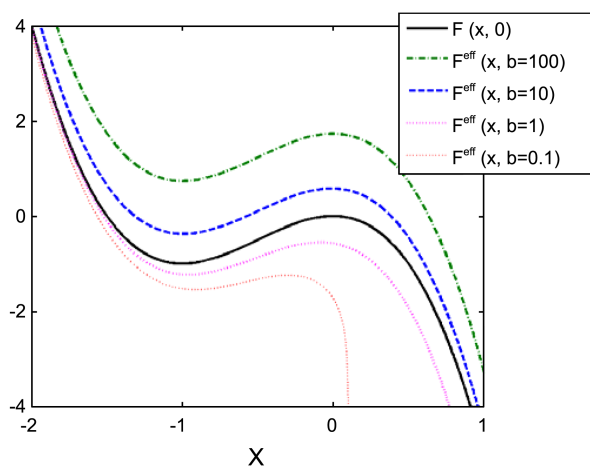


Figure 2. The effective 1D free energy profiles projected from 2D surface for varying b values. $F^{\text{eff}}(x, b)$ deviates from $F(x, 0)$ when $0 < b < 1$.

value should be finite. Therefore, the barrier $F^{\text{eff}}(x, b = 0.1)$ in Figure 2 may be slightly underestimated. However, the exact calculation of $D_{2D}(b, f)$ for $b \rightarrow 0$ leads to a pathological result, in which $D_{2D}(b, f)$ decreases with f . If the behavior of $D_{2D}(b, f)$ at small b is combined with the rest of the term in Eq. (13), $k_{2D}(f)$ exhibits nonmonotonic dependence on f . It is of particular note that even in multidimensional version of Kramers rate expression suggested by Langer, the transition path should be well defined along the multidimensional surface; projecting the 2D surface onto 1D profile leads to a physically incorrect result especially for $b \rightarrow 0$ in which the flat free energy barrier produces no dominant transition path.

As another plausible scenario where the effect of multidimensionality is manifested in the context of force-induced unfolding kinetics, one can study hydrodynamic interaction that dynamically couples the motions along “ x ”- and “ y ”-coordinates. In the presence of hydrodynamic interactions, the mobility tensor \mathbf{M} (Eq. 7) is modified into \mathbf{M}_{HI} with $\gamma_{xy} \neq 0$,

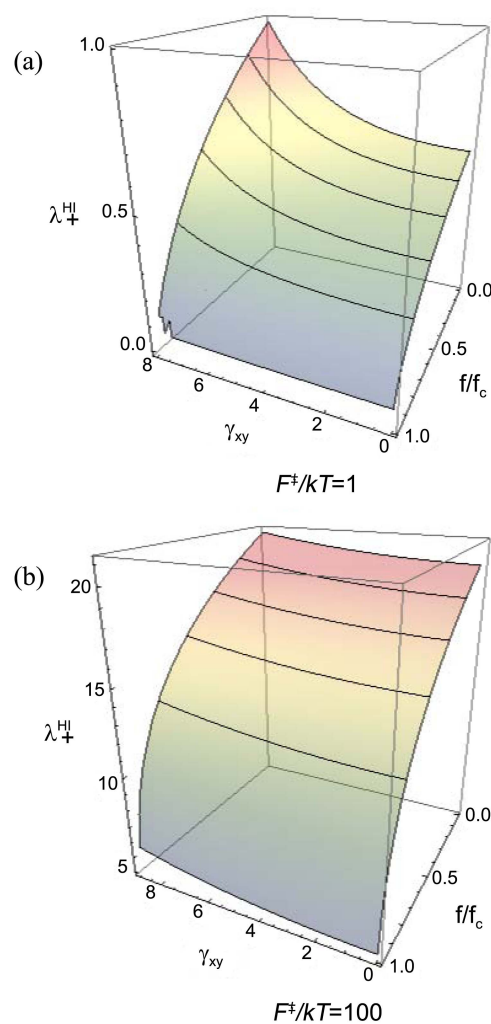


Figure 3. The effect of hydrodynamic interaction (γ_{xy}) on the deterministic growth rate calculated for A. $\beta F^{\ddagger} = 1$ and $\beta F^{\ddagger} = 100$ with other parameters being $\kappa = 1$, $b = 1$, $\gamma_{xx} = \gamma_{yy} = 10$, $x^{\ddagger} = 1$ and $m = 1$.

$$M_{HI} = \begin{pmatrix} 0 & 0 & -1 & 0 \\ 0 & 0 & 0 & -1 \\ 1 & 0 & m\gamma_{xx} & m\gamma_{xy} \\ 0 & 1 & m\gamma_{xy} & m\gamma_{yy} \end{pmatrix} \quad (16)$$

which alters the deterministic growth rate λ_+ into λ_+^{HI} , leaving other terms in $k_{2D}(f)$ (see Eq. 11) unchanged. Since the analytical expression for λ_+^{HI} is quite involved, we obtain λ_+^{HI} numerically by varying γ_{xy} and ff_c and plot $\lambda_+^{HI}(\gamma_{xy}, ff_c)$ in Figure 3. The effect of hydrodynamic interaction on the kinetics through λ_+^{HI} is the most significant when the activation barrier (F^\ddagger) is small. More significantly, pronounced is the variation of λ_{HI} when ff_c is small (see Fig. 3(a)). It is of note that hydrodynamic interactions ($\gamma_{xy} \neq 0$) increases the rate of deterministic divergence from the saddle point ($\lambda_+^{HI} > \lambda_+$), which partially compensates the reduced $D_{2D}(b, f)$ due to large fluctuations.

In order to extract meaningful parameters using 1D profiles, the ensemble of reaction paths should go through a deep and narrow “trough” in the multi-dimensional energy landscape (see $b = 10$ case in Fig. 1), so that fluctuations due to coupling to the auxiliary coordinates is minimal and that the transition path is well defined. Unless this condition is met, the force-induced rupture kinetics in a multidimensional energy landscape can be drastically different from that

inferred from a pre-selected 1D reaction coordinate.

Acknowledgments. This Research was supported by the Chung-Ang University Research Grants in 2008.

References

1. Eyring, H. *J. Chem. Phys.* **1935**, *3*, 107.
2. Evans, M. G.; Polanyi, M. *Trans. Faraday Soc.* **1935**, *31*, 875.
3. Kramers, H. A. *Physica* **1940**, *7*, 284.
4. Grote, R. F.; Hynes, J. T. *J. Chem. Phys.* **1980**, *73*, 2715.
5. Hanggi, P.; Talkner, P.; Borkovec, M. *Rev. Mod. Phys.* **1990**, *62*, 251.
6. Hyeon, C.; Thirumalai, D. *J. Am. Chem. Soc.* **2008**, *130*, 1538.
7. Hyeon, C.; Thirumalai, D. *J. Phys. Cond. Matter* **2007**, *19*, 113101.
8. Greenleaf, W. L.; Frieda, K. L.; Foster, D. A. N.; Woodside, M. T.; Block, S. M. *Science* **2008**, *319*, 630.
9. Bell, G. I. *Science* **1978**, *200*, 618.
10. Dudko, O. K.; Hummer, G.; Szabo, A. *Phys. Rev. Lett.* **2006**, *96*, 108101.
11. Lin, H. J.; Chen, H. Y.; Sheng, Y. J.; Tsao, H. K. *Phys. Rev. Lett.* **2007**, *98*, 088304.
12. Friddle, R. W. *Phys. Rev. Lett.* **2008**, *100*, 138302.
13. Freund, L. B. *Proc. Natl. Acad. Sci. USA* **2009**, *106*, 8818.
14. Hyeon, C.; Morrison, G.; Thirumalai, D. *Proc. Natl. Acad. Sci. USA* **2008**, *105*, 9604.
15. Langer, J. S. *Ann. Phys.* **1969**, *54*, 258.
16. Coffey, W.; Kalmykov, Y. P.; Waldron, J. T. *The Langevin Equation: With Applications to Stochastic Problems in Physics*, 2nd ed.; World Scientific: 2004.